Electroclinic effect in a chiral paranematic liquid-crystal layer above the bulk nematic-to-isotropic transition temperature

Ian R. Nemitz,[1,2,3] Emmanuelle Lacaze,[2,3] and Charles Rosenblatt[1]
[1]*Department of Physics, Case Western Reserve University, Cleveland, Ohio 44106, USA*
[2]*CNRS UMR 7588, Université Pierre et Marie Curie, Institut des NanoSciences de Paris (INSP), 4 place Jussieu, 75005 Paris, France*
[3]*UPMC Université Paris VI, UMR 7588, Institut des NanoSciences de Paris (INSP), 4 place Jussieu, 75005 Paris, France*
(Received 1 December 2015; published 1 February 2016)

Electroclinic measurements are reported for two chiral liquid crystals above their bulk chiral isotropic–nematic phase transition temperatures. It is found that an applied electric field E induces a rotation θ [$\propto E$] of the director in the very thin paranematic layers that are induced by the cell's two planar-aligning substrates. The magnitude of the electroclinic coefficient $d\theta/dE$ close to the transition temperature is comparable to that of a bulk chiral nematic, as well as to that of a parasmectic region above a bulk isotropic-to-chiral smectic-A phase. However, $d\theta/dE$ in the paranematic layer varies much more slowly with temperature than in the parasmectic phase, and its relaxation time is slower by more than three orders of magnitude than that of the bulk chiral nematic electroclinic effect.

DOI: 10.1103/PhysRevE.93.022701

I. INTRODUCTION

Several decades ago Miyano, and then Tarczon and Miyano, demonstrated the growth of surface-induced orientational order on cooling a liquid crystal toward the isotropic-to-nematic phase transition temperature T_{IN} [1,2]. In their experiments they measured the total optical phase retardation through the cell, which derives from this thin "paranematic" region, as a function of the cell's surface treatment. There has been a tremendous amount of activity since this initial work, both theoretical and experimental, aimed at measuring and understanding the growth of orientational order at a bounding substrate [3–25]. In nearly all cases it had been assumed that the potential is localized near, i.e., within a few nanometers of, the liquid crystal–alignment layer interface [3,5,9–11]. If the interaction is weak, only partial wetting of the nematic phase occurs. On the other hand, for sufficiently strong interactions, the nematic phase completely wets the surface and the integrated orientational scalar order parameter S diverges logarithmically on cooling toward T_{IN} [1–3,12]. Here $S \equiv \langle \frac{3}{2}\cos^2\varphi - \frac{1}{2}\rangle$, where φ is the orientation of the liquid-crystal molecule. Other phenomena such as capillary condensation in which a localized boundary layer transitions to the nematic phase [4,11,13,14,18–20], and a prewetting transition in which the orientational order parameter increases discontinuously at a temperature just above T_{IN} [5,23], have been predicted theoretically and observed experimentally. More recently Lee *et al.* immersed a highly tapered optical fiber into a thin paranematic layer above T_{IN} and determined the surface-induced orientational order parameter $S(z)$ as a function of temperature and height z above the substrate [24]. Their analysis was model free; i.e., it did not require a specific functional form for the spatial decay of the order. They found that S initially decays weakly with z into the bulk for $z < 10\,\mathrm{nm}$, after which it falls off rapidly with increasing z. Pikina and Rosenblatt explained the results theoretically in terms of the small isotropic-nematic (IN) interfacial tension and a resulting renormalization of the repulsive interactions from fluctuations of the IN interface [25].

Turning to chirality, it long has been known that an electroclinic effect (ECE) occurs in a bulk chiral smectic-A (Sm-A*) phase in which mirror symmetry is broken and a C_2 symmetry axis lies parallel to the smectic layer plane [26]. Application of an electric field E establishes the specific C_2 axis and results in a director rotation by an angle $\theta[\propto E]$ about that axis. Although an ECE has been observed in the bulk chiral nematic phase [27,28], the required symmetry is due to the existence of smectic layer fluctuations. That is, the bulk chiral nematic ECE is due to smectic fluctuations in the chiral nematic phase [29].

At a liquid crystal–substrate interface, one may find an analogous rotation proportional to the applied field; this is the so-called *surface* ECE [30–33]. There are two conditions: (i) The required chiral environment can be due to either liquid-crystal chirality or surface chirality—or both, and (ii) the required reduced rotational symmetry is due to the existence of an easy axis for planar alignment and the subsequent reduction of symmetry from a C_∞ to a C_2 rotation axis perpendicular to the surface [34]. This easy axis typically is created by rubbing the substrate or polarized UV light exposure of the polymer alignment layer. Thus a surface ECE has been observed for chiral surfaces and an achiral liquid crystal [34–36], and for an achiral surface with an easy axis and a chiral liquid crystal [33].

To observe the surface ECE in a bulk achiral nematic phase, an electric field E is applied perpendicular to the chiral substrate and results in a torque on the director at the substrate. In consequence the surface director rotates in a plane perpendicular to the electric field vector, with competing viscoelastic torques from the surface easy axis (the anchoring torque) and bulk liquid crystal opposing this rotation. In quasiequilibrium the bulk liquid-crystal director (away from the surface) is rotated elastically by the liquid-crystal surface region [35,36]. The magnitude of this surface electroclinic coefficient $e_c = d\theta/dE$ depends on the chemistry of the liquid crystal, its dipole moment, and the coupling between the liquid crystal and the substrate's easy axis [34]. However, a necessary ingredient for the existence of a surface ECE is chirality at the interface. When the surface is chiral, the ECE can be used as a metric of the strength of chiral induction from the chiral surface into the configurationally achiral liquid crystal. When the surface is not chiral but has an easy axis, an ECE in a bulk chiral smectic-A has been demonstrated

[33]. Here we are interested in an achiral substrate and chiral nematic liquid crystal, but *above* the bulk T_{IN}, where only a thin orientationally ordered layer exists close to the substrate.

An ECE study in the isotropic phase has been performed previously for chiral liquid-crystal molecules that present a chiral smectic-*A* (Sm-*A**) phase, with no chiral nematic phase present. In this work Lee *et al.* examined a chiral liquid crystal in the bulk isotropic phase in a cell whose surfaces were treated for planar alignment [37]. On cooling toward a direct isotropic-to-Sm-*A** (IA) transition having no intermediate nematic phase, they observed not only a thin region (of characteristic thickness a few nanometers) of surface-induced smectic order, but also observed a surface ECE: Application of an electric field resulted in a rotation of the director proportional to E. In their case, however, there was no elastic transmission of the director rotation into the bulk liquid crystal, as the bulk was disordered, i.e., in the isotropic phase. That a surface region of smectic can exist even at bulk isotropic temperatures is not surprising, and has been shown explicitly by several groups [19,38,39]. The ECE results of Lee *et al.* [37] exhibit a dramatic temperature dependence in which e_c increases by nearly three orders of magnitude when the temperature is reduced by 1 K in the isotropic phase, from $T_{IA} + 1.2$ K to $T_{IA} + 0.2$ K, where T_{IA} is the isotropic–Sm-*A** phase transition temperature. (Their lowest temperature reported was $T_{IA} + 0.2$ K.) They noted that this rapid temperature variation is indicative of the appearance of incipient smectic layers at the substrate in an otherwise bulk isotropic phase [37]. Moreover, they explicitly *excluded* the possibility of only nematic order in this thin surface region close to T_{IA}, except perhaps immediately adjacent to, i.e., within 1 nm of, the substrate.

As noted above, a surface ECE has been observed at temperatures in the nematic phase [32,35,36]. Importantly, smectic fluctuations near the substrate are not required for this effect to occur: The reduced symmetry at the surface, along with chirality at the surface, is sufficient to generate a surface ECE in the nematic phase [34]. The purpose of this work is to address the question of what occurs *above* the bulk isotropic-chiral nematic phase transition temperature on cooling the liquid crystal toward T_{IN}. We know that a thin layer of oriented liquid crystal, perhaps $h = 10$–20 nm, appears at the substrate(s) [24], with a characteristic thickness h that depends on the nature of the surface, the liquid crystal, and T–T_{IN}. Moreover, the profile of the order parameter S vs z tends not to be a decaying exponential, but exhibits a shoulder [24], thus facilitating the simple approximation of a uniformly oriented paranematic region of thickness h extending a short distance $h(T–T_{IN})$ from the surface, beyond which the liquid crystal can be considered as isotropic. Here we report on temperature- and frequency-dependent measurements of an electroclinic effect in this thin paranematic region of a chiral liquid crystal above the bulk isotropic-to-chiral nematic—this is sometimes referred to as "cholesteric"—phase transition temperature. Our central results are as follows: An ECE is observed and grows continuously with decreasing temperature before being cut off by a first order phase transition at T_{IN}; the rate of growth with decreasing temperature, viz., $|de_c/dT|$, is *much* more gradual than was observed in a thin chiral parasmectic region by Lee *et al.* [37]; and a relaxation frequency is in the neighborhood of several hundred hertz, which is slower by many orders of magnitude than the frequency response in the bulk nematic electroclinic effect, yet faster than a surface-driven ECE into a bulk nematic phase [40].

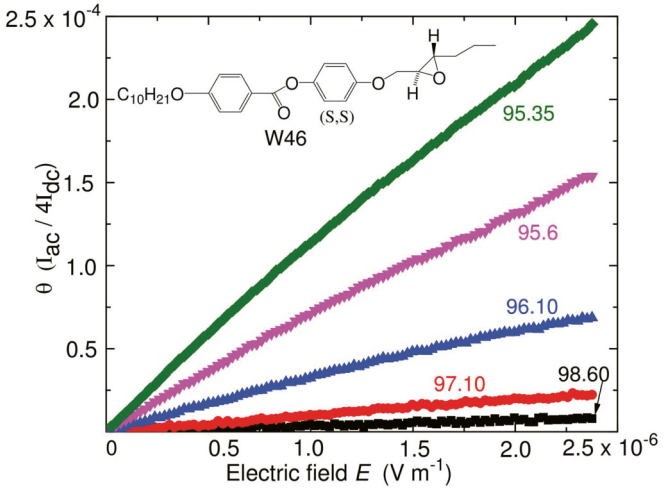

FIG. 1. $I_{ac}/4\,I_{dc}$, which is defined as the effective rotation angle θ, vs applied electric field E for the liquid crystal W46 (shown) at several temperatures above the bulk isotropic–nematic transition temperature. The structure of W46 is shown.

II. EXPERIMENT

Capacitive cells were prepared using indium-tin-oxide (ITO) coated glass substrates that were spin coated with the planar alignment agent RN-1175 polyamic acid (Nissan Chemical Industries). The coated substrates were prebaked for 5 min at 80 °C and then baked for 60 min at 250 °C. The polyimide surfaces were rubbed unidirectionally with a cotton pile cloth (YA-20-R, Yoshikawa Chemical Co., Ltd.) attached to the cylindrical roller of an Optron rubbing machine to generate an easy axis for planar liquid-crystal director alignment. The rubbed substrates were placed together in an antiparallel geometry, separated by Mylar spacers, and cemented to form cells of a thickness of several micrometers. The empty-cell thicknesses d were measured by interferometry, as d is required to determine the electric field magnitude E from the applied voltage V. Conducting leads were attached to the ITO and the cells were filled in the isotropic phase via capillary action with negative dielectric anisotropy chiral liquid crystals (LCs). One liquid crystal was the single component (*S*,*S*) enantiomer of W46 (Displaytech, Inc.), for which the manufacturer specifies the phase sequence *I*–97°–*N**–81°–Sm-*A**–80°–Sm-*C**–75°–Cry and is shown in the inset of Fig. 1. Here the asterisks signify that the liquid-crystalline phases are chiral. W46 shows virtually no biphasic region around the IN transition temperature T_{IN} and has a 16–17 K wide *N** phase. The other material was the chiral mixture SCE12 (Merck, formerly BDH Ltd.), which has a manufacturer-specified phase sequence *I*–118°–*N**–81°–Sm-*A**–66°–Sm-*C**. This material, although having a biphasic region, has an extremely wide *N** range of some 37 K. Moreover, there is a large extant literature for its bulk chiral ECE with which we can compare our results. The cells were inserted into an oven that was temperature

stabilized to 20 mK, which then was placed in a classic electroclinic optical setup [41], where light from a power stabilized diode laser ($\lambda = 532$ nm) passed through a polarizer oriented at 22.5° with respect to the cell's rubbing easy axis, through the cell, and then through a crossed polarizer. The light intensity was detected with a photodiode detector, for which we previously had measured a calibration curve $C(f)$ for the detector and lock-in amplifier combination. $C(f)$, which was determined by exposing the detector and downstream electronics to light from a light emitting diode over the frequency range $1 < f < 10^5$ Hz, was found to be flat to within a few percent over the frequency range used in our experiments; nevertheless, for consistency all intensities were scaled by $C(f)$. The cells' temperatures were raised by at least 30 °C above their respective T_{IN} and the optics were adjusted to extinguish almost fully the intensity of the laser light passing through the crossed polarizers. A small remnant signal was due to the weak paranematic region near the substrates as well as to the small strain birefringence in the optics. The consequence of this background will be discussed below. We note that owing to the extreme thinness of the paranematic region relative to the pitch of the chiral nematic helix, we can treat the director orientation in the paranematic region as being nearly uniform.

The electroclinic coefficient $e_c = d\theta/dE$ was measured for the single-component W46 liquid crystal as a function of temperature at fixed frequency $f = 1000$ Hz, and also as a function of frequency at several temperatures above the bulk nematic–isotropic transition temperature $T_{IN} \sim 95.2 \pm 0.2$ °C, which is slightly different than the manufacturer's specifications. We determined the transition temperature from texture measurements, as well as the extremely sharp increase of our optical signal (see below). For all measurements, an ac electric field was applied across the cells, and the detector output was fed into both a dc voltmeter and a lock-in amplifier that was referenced to the ac driving frequency f. For the first set of scans, the W46 cell was brought deep into the isotropic phases (>11 K above the IN transition) and an ac electric field was applied across the cell at $f = 1000$ Hz. The rms voltage V was stepped upward from 0 to 5 V over 400 s with a 4-s dwell time between each measurement, the intensity scaled by $C(f)$, and both the scaled ac intensity I_{ac} and scaled dc intensity I_{dc} were recorded. Here I_{ac} is the intensity at the detector measured by the lock-in amplifier at driving frequency f and I_{dc} is the dc component of intensity measured by a digital voltmeter. The temperature T then was reduced and another voltage scan was made, with temperature increments becoming smaller as T approached T_{IN}. Figure 1 shows the quantity $I_{ac}/4I_{dc}$, which corresponds to the effective rotation angle θ in the surface paranematic regions [41], vs applied field at several temperatures. The reason that we use the word "effective" in defining the rotation angle is because the orientational order parameter S is not completely uniform through the paranematic region, and therefore θ may vary with position. Figure 2 shows the derivative with respect to electric field E of the data in Fig. 1, which is defined as an effective electroclinic coefficient $e_c = d\theta/dE = d(I_{ac}/4I_{dc})/dE$. (The inset shows $1/e_c$ vs temperature.) Similar measurements also were performed on cells containing the chiral liquid-crystal mixture SCE12, with the results shown in Fig. 3. Because of phase separation at the isotropic-to-nematic transition in SCE12, we do not attempt to identify a transition temperature T_{IN}. Instead, we simply show the SCE12 results for e_c vs temperature in Fig. 3.

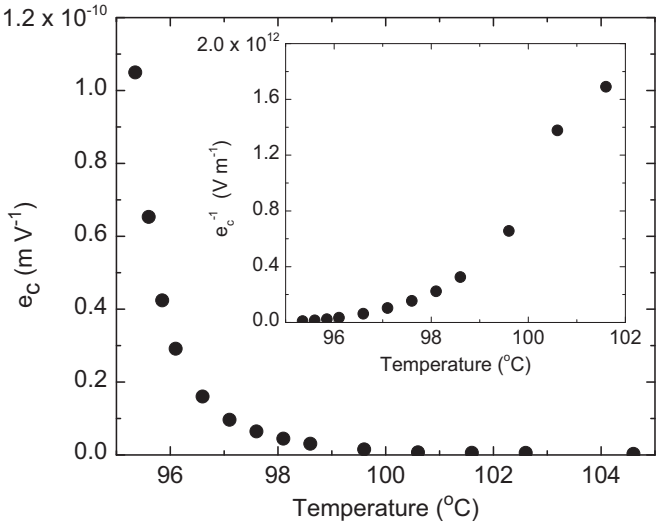

FIG. 2. The effective electroclinic coefficient e_c vs temperature for W46. The inset shows the inverse electroclinic coefficient e_c^{-1} vs temperature.

For the second scan, the temperature of the W46 liquid crystal was fixed at four different values $\Delta T [= T - T_{IN}]$ relative to T_{IN} : $\Delta T = 0.7$, 1.2, 1.7, and 2.2 K. A constant electric field $E = 4.8\,\mathrm{V\,m^{-1}}$ was applied as the frequency was varied over 3000 s from 40 Hz to 40 kHz in logarithmic steps, with a 12-s dwell time at each data point. Figure 4 shows e_c vs f, using a linear vertical scale in Fig. 4(a) and a logarithmic scale in Fig. 4(b). We need to point out that because of the extraordinarily small integrated birefringence in the ultrathin paranematic region, we had to contend with (possibly temperature-dependent) small offset values of I_{dc} from the inherent birefringence in the optics. This offset resulted in a systematic error in e_c (generally downward) of a few percent

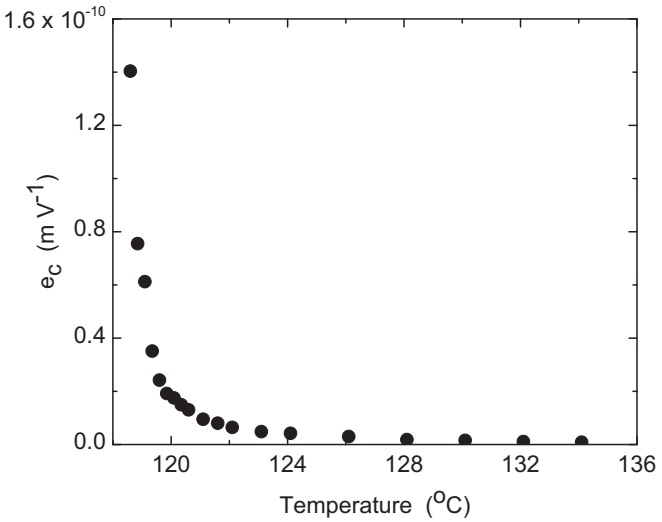

FIG. 3. The effective electroclinic coefficient e_c vs temperature for SCE12.

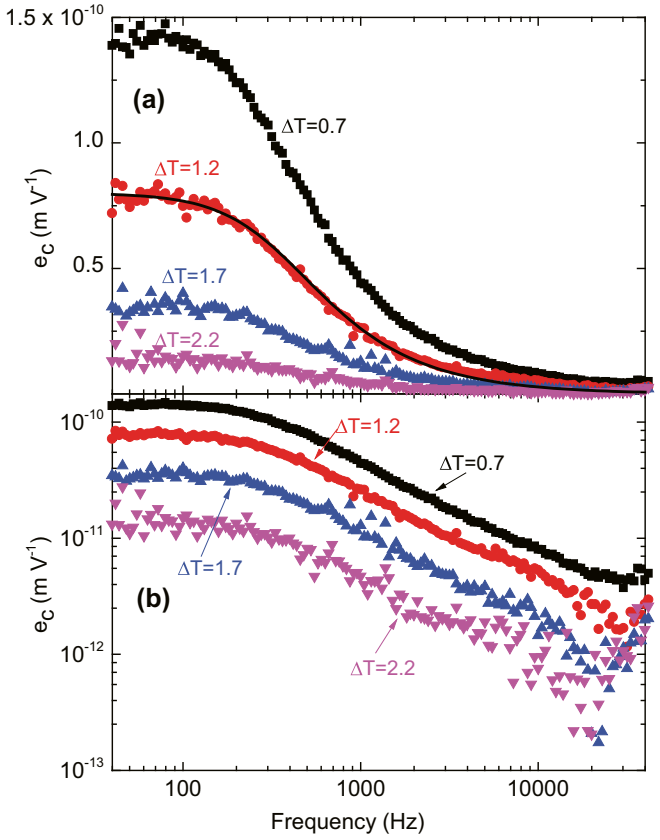

FIG. 4. (a) The electroclinic coefficient measured for W46 as a function of frequency f at four temperatures ΔT above $T_{\rm IN}$. A fit to the Debye form is shown for $\Delta T = 1.2$ K. (b) Same as (a) but using a logarithmic scale for e_c.

within a quarter degree of the transition temperature $T_{\rm IN}$, of ∼20% within a degree of $T_{\rm IN}$, and considerably more several degrees above $T_{\rm IN}$. At $T > T_{\rm IN} + 4$ K the (unwanted) background in $I_{\rm dc}$ was comparable to the (desired) component from the integrated birefringence in the paranematic layer, indicating that e_c could be in error by a factor of 2. Nevertheless, despite this systematic error, the general trends observed in our data permit us to make strong conclusions about the physics, especially close to $T_{\rm IN}$.

III. RESULTS AND DISCUSSION

Let us first examine the $f = 1000$ Hz electroclinic data for the single-component liquid crystal W46, as shown in Fig. 2. Here $T_{\rm IN} = (95.2 \pm 0.2)\,^{\circ}$C, which occurs approximately 16 K above the N^*–Sm-A^* phase transition temperature and 17 K above the Sm-A^*–Sm-C^* transition temperature. As noted above, the data at higher temperatures have larger relative uncertainties and systematic errors than those close to $T_{\rm IN}$ owing to the very small values of both $I_{\rm ac}$ and $I_{\rm dc}$ far above $T_{\rm IN}$. As is evident in Fig. 2, e_c increases smoothly with decreasing temperature, with the magnitude of e_c close to $T_{\rm IN}$ being similar to that of Ref. [37] close to the Sm-A^*–isotropic transition. This increase of e_c with decreasing temperature close to the transition derives primarily from the increasing order parameter S on approaching $T_{\rm IN}$. But other effects also may come into play. First, the thickness h of the paranematic region near the surface increases as the liquid crystal is cooled toward $T_{\rm IN}$ [1,2,24]. This growth of h increases *both* $I_{\rm ac}$ and $I_{\rm dc}$ by the same total optical retardation factor. Thus, in principle $e_c = d(I_{\rm ac}/4I_{\rm dc})/dE$ is minimally affected by the temperature-dependent width h of the paranematic region, except insofar as the order parameter S and coupling to the symmetry-breaking surface depend more strongly on z when h becomes larger close to the IN transition. Second, the frequency dependence of the electroclinic effect is quite strong, as is apparent in Figs. 4(a) and 4(b). We chose to collect data in Fig. 2 at frequency $f = 1000$ Hz—this frequency is the same used by Lee *et al.* [37]—because the signal-to-noise ratio is considerably better than it is at lower frequencies. But our choice of $f = 1000$ Hz, which is well above the quasi-dc region that extends out to several hundred hertz (Fig. 4), could possibly confound our interpretation of e_c vs T in Fig. 2: *If* our measured e_c vs f profile [Figs. 4(a) and 4(b)] were temperature dependent in ways beyond a simple multiplicative factor, e.g., if there were a critical slowing down near $T_{\rm IN}$, then the shape of our measured e_c vs T curve would depend on frequency. However, our e_c vs temperature measurements in Fig. 4 [and especially in the logarithmic plot Fig. 4(b)] indicate that all e_c vs T curves are nearly identical, aside from a multiplicative factor associated with the rotational susceptibility vs temperature. This suggests that there is little or no slowing down near the transition temperature, and thus the shape of the e_c vs T curve in Fig. 2 is approximately independent of frequency, aside from a scaling factor that decreases with increasing f, as seen in Figs. 4(a) and 4(b). Herein, therefore, lies an important difference with the parasmectic effect in Ref. [37]: Whereas Ref. [37] reports a nearly three orders of magnitude increase in the electroclinic effect on decreasing the temperature from $T = T_{\rm IA} + 1.2$ K to $T = T_{\rm IA} + 0.2$ K, for our sample the analogous increase above $T_{\rm IN}$ is only one order of magnitude (Fig. 2). Lee *et al.* ascribed [37] their very rapid variation of e_c with temperature in the parasmectic region to the strong temperature dependence of the smectic order parameter, even if an ultrathin (one or two molecules) of only nematic order resided immediately at the interface. To be sure, the liquid crystals used herein and in Ref. [37] are not the same. Nevertheless, the very large difference in their respective temperature profiles is quite remarkable, and shows a very different sort of qualitative behavior between a paranematic and parasmectic region.

We make another observation based on the data in Fig. 2. The inset in Fig. 2 shows the inverse response, i.e., e_c^{-1}, vs temperature. The IN transition generally exhibits mean-field-like behavior in quantities such as the Kerr [42,43] or Cotton-Mouton [44] coefficient above $T_{\rm IN}$, where the relevant response function at wave vector $q = 0$ varies as $(T - T_{IN})^{-1}$. There can be small variations from this form very close to the transition, generally involving a small downward deviation of the inverse susceptibility. However, the inset in Fig. 2 clearly shows a deviation opposite from those found elsewhere [42–44]. Although the induced order parameter S at the surface has been shown to increase in a mean-field-like manner [24], the chiral coupling with the substrate and the anchoring strength coefficient both play a role in the surface ECE response [34]. Our results thus suggest that the evolution of the ECE with

temperature goes beyond the evolution of S and also involves the evolution of chiral coupling with the substrate and/or the anchoring strength coefficient. The temperature dependences of these quantities, which are beyond the scope of this work, have not yet been determined. Nevertheless, the observed deviation near T_{IN} of the ECE from mean-field behavior is a potentially fertile area for future study.

We now consider Figs. 4(a) and 4(b), the frequency response of W46 above T_{IN}. The behavior is close to that of a single relaxation process having a Debye-like response $\theta = kE/[D(1+\eta^2\omega^2/D^2)^{1/2}]$. Here k is the coupling constant between θ and E in the free energy, which can depend on the anchoring strength coefficient W_2^{φ} [34]; η is a viscosity; $\omega = 2\pi f$; and D is an inverse tilt susceptibility with respect to the easy axis and is proportional to W_2^{φ}. (Note that D would correspond to an inverse tilt susceptibility relative to the layer normal for a bulk liquid crystal above the Sm-A* to Sm-C* transition temperature.) We fitted the data in Fig. 4(a) at $\Delta T = 1.2$ K, as shown, and found a relaxation time of $\tau = (2\pi f)^{-1} = (4.5 \pm 0.4) \times 10^{-4}$ s. The same relaxation time τ is obtained when fitting data at the other temperatures, which also can be seen in the log-log plot shown in Fig. 4(b), where the curves are identical except for a vertical translation. Therefore we conclude that τ shows no significant temperature dependence over the temperature range studied. Single-relaxation Debye behavior often is observed in a bulk ECE in the Sm-A* and chiral nematic phases [26,40,45]. The relaxation time τ_{bulk} for the bulk chiral nematic electroclinic effect is fast, typically $\tau_{bulk} < 10^{-6}$ s [40]. However, surface nematic electroclinic effects due to chirality localized at a surface tend to be *much* slower [45–47]. In particular, the e_c vs frequency data in Ref. [47] corresponds to a bulk *achiral* nematic liquid crystal that becomes deracemized immediately adjacent to the polymer alignment layer. An electric field thus drives a rotation of the director at the surface, which in turn is transmitted by elastic forces into the bulk. Thus the frequency response in that experiment is related to dissipation at the liquid crystal–polymer interface, but also (and importantly) to the viscosity for twistlike elastic distortions in the bulk liquid crystal. It is interesting that our e_c vs f data shown in Figs. 4(a) and 4(b) are much slower than τ_{bulk}, but much faster than nematic ECEs driven by the surface [45–47]. We believe that the relaxation process in Figs. 4(a) and 4(b) is due primarily to dissipation from the director rotation at the surface, but is not slowed further by elastic coupling to the (now nonexistent) bulk nematic region, as was the case for a surface-driven process at the interface between a bulk nematic liquid crystal and chiral period mesoporous organosilica [45].

Let us now turn to the data for SCE12, which are shown in Fig. 3. SCE12 is a (proprietary) mixture and therefore phase separates at the isotropic–chiral nematic transition, rendering it less ideal for this study. Nevertheless, we have examined SCE12 for two important reasons: (i) SCE12 has a very large nematic phase range—$T_{IN} \sim T_{NA} + 37$ K—so that smectic fluctuations at temperatures above T_{IN} are virtually nonexistent, and (ii) comparisons can be made with the large extant literature for its bulk chiral nematic and Sm-A* electroclinic effects. We note that we easily verified that measurements were performed in the isotropic phase rather than the biphasic region by monitoring I_{dc}, which jumped immediately by several orders of magnitude on cooling into the biphasic region. We first compare the approximate magnitude of our surface ECE with that of Lee *et al.* [37] at temperatures a few hundred millikelvins above their respective phase transition temperatures, viz., T_{IN} and T_{IA}. Note that Ref. [37] reports results for I_{ac}/I_{dc}, which is a factor of 4 larger than our definition of $\theta = I_{ac}/4I_{dc}$. Accounting for this difference, in Fig. 3 we find values for $e_c \sim 10^{-11}$ to 10^{-10} rad V^{-1} m at a temperature a few hundred millikelvins above T_{IN} for SCE12. This is smaller than—but of the same order of magnitude as—the data reported in Ref. [37] at comparable temperatures above T_{IA}. That the surface ECE is a bit smaller above the N*–isotropic transition than it is above a direct Sm-A*–isotropic transition [37] is not surprising: The "strength" of the symmetry breaking due to the substrate's easy axis in the former case, and the strength of the induced smectic order in the latter, both depend critically on the surface preparation and choice of liquid crystals. We also can compare the *surface* ECE data in Fig. 3 for the liquid crystal SCE12 with previous measurements of the ECE for SCE12 in the *bulk* nematic phase [28]. In Fig. 3 we find a value of $e_c \sim 10^{-10}$ rad V^{-1} m for SCE12 in the paranematic region just above T_{IN}. This is of the same order found for its bulk ECE nearly 37 K lower in temperature, deep into the *bulk* chiral nematic phase and only 0.3 K above the Sm-A* to N* transition temperature T_{NA} [28]. This suggests that smectic order is extremely unlikely to be playing a role in our *surface* ECE measurements above T_{IN} presented herein because $T_{IN} = T_{NA} + 37$ K. In fact, at $T_{NA} + 9$ K, corresponding to ~28 K below T_{IN}—this is the highest temperature examined in Ref. [28]—the bulk nematic e_c for SCE12 [28] already is more than an order of magnitude smaller than the value reported herein for the surface ECE just above the IN phase transition temperature T_{IN}.

Pretransitional phenomena at a liquid crystal–substrate interface are rich in physics. Based upon our understanding that a chiral electroclinic effect obtains at a substrate having an easy axis for orientation, and does *not* require smectic layering [34], we demonstrated an electroclinic effect in the thin paranematic layer above the bulk chiral nematic–isotropic phase transition temperature. We found that the magnitude of the response near the transition temperature is comparable to that of a parasmectic region just above the Sm-A*–isotropic transition temperature, but falls off much more slowly with increasing temperature above the transition than that in the parasmectic layer [37]. Moreover, the magnitude in the paranematic layer is similar to that in the bulk chiral nematic phase just above the transition to the Sm-A* phase. But unlike the bulk nematic phase, the electroclinic effect in the paranematic phase has a relaxation time that is about three orders of magnitude slower.

ACKNOWLEDGMENTS

I.R.N. and C.R. were supported by the National Science Foundation's Condensed Matter Physics program under Grant No. DMR-1505389. I.R.N., C.R., and E.L. are grateful to the Partner University Fund, administered by the French Foreign Ministry, for supporting travel between, and residential costs in, Paris and Cleveland.

[1] K. Miyano, Phys. Rev. Lett. **43**, 51 (1979); J. Chem. Phys. **71**, 4108 (1979).
[2] J. C. Tarczon and K. Miyano, J. Chem. Phys. **73**, 1994 (1980).
[3] D. W. Allender, G. L. Henderson, and D. L. Johnson, Phys. Rev. A **24**, 1086 (1981).
[4] P. Sheng, Phys. Rev. Lett. **37**, 1059 (1976).
[5] P. Sheng, Phys. Rev. A **26**, 1610 (1982).
[6] H. Hsiung, Th. Rasing, and Y. R. Shen, Phys. Rev. Lett. **57**, 3065 (1986).
[7] W. Chen, L. J. Martinez-Miranda, H. Hsiung, and Y. R. Shen, Phys. Rev. Lett. **62**, 1860 (1989).
[8] M. B. Feller, W. Chen, and Y. R. Shen, Phys. Rev. A **43**, 6778 (1991).
[9] T. Moses and Y. R. Shen, Phys. Rev. Lett. **67**, 2033 (1991).
[10] T. J. Sluckin and A. Poniewierski, in *Fluid Interfacial Phenomena*, edited by C. A. Croxton (John Wiley & Sons Ltd, Chichester, UK, 1986), p. 215.
[11] T. J. Sluckin and A. Ponewierski, Liq. Cryst. **2**, 281 (1987).
[12] B. Jérôme, Rep. Prog. Phys. **54**, 391 (1991).
[13] H. Yokoyama, S. Kobayashi, and H. Kamei, Mol. Cryst. Liq. Cryst. **99**, 39 (1983).
[14] H. Yokoyama, S. Kobayashi, and H. Kamei, J. Appl. Phys. **61**, 4501 (1987).
[15] G. Barbero and G. Durand, J. Phys. II (Paris) **1**, 651 (1991).
[16] R. Barberi and G. Durand, Phys. Rev. A **41**, 2207 (1990).
[17] S.-T. Wu and U. Efron, Appl. Phys. Lett. **48**, 624 (1986).
[18] A. Borštnik Bračič, K. Kočevar, I. Muševič, and S. Žumer, Phys. Rev. E **68**, 011708 (2003).
[19] K. Kočevar, A. Borštnik, I. Muševič, and S. Žumer, Phys. Rev. Lett. **86**, 5914 (2001).
[20] K. Kočevar and I. Muševič, Phys. Rev. E **64**, 051711 (2001).
[21] B. Wen, J.-H. Kim, H. Yokoyama, and C. Rosenblatt, Phys. Rev. E **66**, 041502 (2002).
[22] J.-H. Kim and C. Rosenblatt, J. Appl. Phys. **84**, 6027 (1998).
[23] X. Liu, D. W. Allender, and D. Finotello, Europhys. Lett. **59**, 848 (2002).
[24] J.-H. Lee, T. J. Atherton, V. Barna, A. De Luca, E. Bruno, R. G. Petschek, and Ch. Rosenblatt, Phys. Rev. Lett. **102**, 167801 (2009).
[25] E. Pikina and C. Rosenblatt, Eur. Phys. J. E **35**, 87 (2012).
[26] S. Garoff and R. B. Meyer, Phys. Rev. Lett. **38**, 848 (1977).
[27] Z. Li, R. G. Petschek, and C. Rosenblatt, Phys. Rev. Lett. **62**, 796 (1989).
[28] Z. Li, G. A. Di Lisi, R. G. Petschek, and C. Rosenblatt, Phys. Rev. A **41**, 1997 (1990).
[29] J. Etxebarria and J. Zubia, Phys. Rev. A **44**, 6626 (1991).
[30] K. Nakagawa, T. Shinomiya, M. Koden, K. Tsubota, T. Kuratate, Y. Ishii, F. Funada, M. Matsura, and K. Awane, Ferroelectrics **85**, 39 (1988).
[31] J.-Z. Xue and N. A. Clark, Phys. Rev. Lett. **64**, 307 (1990).
[32] S. Tripathi, M.-H. Lu, E. M. Terentjev, R. G. Petschek, and C. Rosenblatt, Phys. Rev. Lett. **67**, 3400 (1991).
[33] J. E. Maclennan, D. Muller, R.-F. Shao, D. Coleman, D. J. Dyer, D. M. Walba, and N. A. Clark, Phys. Rev. E **69**, 061716 (2004).
[34] R. Basu, I. R. Nemitz, Q. Song, R. P. Lemieux, and C. Rosenblatt, Phys. Rev. E **86**, 011711 (2012).
[35] S. Ferjani, Y. Choi, J. Pendery, R. G. Petschek, and C. Rosenblatt, Phys. Rev. Lett. **104**, 257801 (2010).
[36] J. Pendery, S. Ferjani, C. Rosenblatt, and R. G. Petschek, Eur. Phys. Lett. **96**, 26001 (2011).
[37] S.-D. Lee, J. S. Patel, and J. W. Goodby, Phys. Rev. A **44**, 2749 (1991).
[38] W. Chen, Y. Ouchi, T. Moses, Y. R. Shen, and K. H. Yang, Phys. Rev. Lett. **68**, 1547 (1992).
[39] T. Moses, Y. Ouchi, W. Chen, and Y. R. Shen, Mol. Cryst. Liq. Cryst. **225**, 55 (1993).
[40] Z. Li, R. Ambigapathy, R. G. Petschek, and C. Rosenblatt, Phys. Rev. A **43**, 7109 (1991).
[41] G. Andersson, I. Dahl, P. Keller, W. Kuczynski, S. T. Lagerwall, K. Skarp, and B. Stebler, Appl. Phys. Lett. **51**, 640 (1987).
[42] A. R. Johnson, J. Appl. Phys. **44**, 2971 (1973).
[43] J. C. Filippini and Y. Poggi, J. Phys. Lett. **35**, L99 (1974).
[44] T. W. Stinson, J. D. Litster, and N. A. Clark, J. Phys. Colloq. **33**, C1-69 (1972).
[45] I. R. Nemitz, K. McEleney, C. M. Crudden, R. P. Lemieux, R. G. Petschek, and C. Rosenblatt, Liq. Cryst. (2016).
[46] I. M. Syed and C. Rosenblatt, Phys. Rev. E **67**, 041707 (2003).
[47] R. Basu, J. S. Pendery, R. G. Petschek, R. P. Lemieux, and C. Rosenblatt, Phys. Rev. Lett. **107**, 237804 (2011).